DMD Fast Forward. Published on March 2, 2005 as doi:10.1124/dmd.104.002592

The Distribution, Metabolism, and Elimination of Clofarabine in Rats

Peter L. Bonate, Larry Arthaud, John Stuhler, Phyllis Yerino, Randall J. Press,

and James Q. Rose

Affiliations:

Genzyme Oncology, 4545 Horizon Hill Boulevard, San Antonio, TX 78229 USA (PLB, LA)
Quintiles, 10245 Hickman Mills Drive, Kansas City, MO 64137 USA (JS, RJP, JQR, PY)
Current affiliation: XenoTech, 16825 W 116th Street, Lenexa, KS 66219 USA (PY)

Running Title: Pharmacokinetics of Clofarabine in Rats

Corresponding Author (PB):
email: peter.bonate@genzyme.com
phone: 210-949-8662
fax: 210-949-8219

Nonstandard Abbreviations:

DLT, dose limiting toxicity; DMEM, Dubecco's Modified Eagle Medium; GLP, good laboratory practices; DRR, daily recovery of radioactivity; MTD, maximum tolerated dose; ROI, region of integration; QWBA, quantitative whole body autoradiography.

Word Count Abstract: 256
Word Count Introduction: 431
Word Count Discussion: 602
Tables and Figures: 8
Total Word Count: 6804
Page Count: 29
Number of References: 8

Abstract

The distribution, metabolism and elimination of intravenous 14C-clofarabine was studied in Fischer 344 male rats under a once daily for 5 days dosing schedule of 25 or 50 mg/kg/day. Also, the *in vitro* metabolism in rat, dog, and human hepatocytes was studied. Plasma radioactivity (of which clofarabine accounted for 63% to 93%) exhibited three phases of exponential elimination with half-lives of 0.3, 1.3, and 12.8 hours after administration of the 25 mg/kg/d regimen. Unscheduled deaths occurred after 1 to 3 doses with the 50 mg/kg regimen, possibly due to nonlinear pharmacokinetics, and so mass balance and radiokinetic profiles could not be obtained. A total of 77.1% (of which 87.2% was clofarabine) and 10.8% (of which 6.9% was clofarabine) of the dose was recovered in urine and feces, respectively. 6-ketoclofarabine, believed to be formed via adenosine deaminase, was the metabolite of greatest concentration found in urine and feces, but in each matrix accounted for only 7% of the daily recovery of radioactivity. 6-ketoclofarabine was also found in myocardium and liver, but accounted for less than 2% of the total radioactivity in those tissues. Clofarabine was the major analyte found in myocardium (> 97% region of integration) and liver (> 94% region of integration). Whole body autoradiography demonstrated that the highest postdistributive concentrations of radioactivity were in the excretory organs, kidney, bladder and GI tract, with no remarkable suborgan distribution. In rat, dog, and human hepatocytes, 95, 96, and 99.8%14C-clofarabine remained, respectively, after 6 hours incubation. Eleven metabolites were observed with the largest constituting 2.5% of the radioactivity.

Introduction

Clofarabine (Figure 1; 2-chloro-2'-fluoro-deoxy-9-β-D-arabinofuranosyladenine) is a next-generation nucleoside analog being developed for the treatment of solid and hematologic tumors. Clofarabine is a nucleoside prodrug that must be intracellularly metabolized to its mono-, di-, and then, finally, triphosphate conjugate for activity to be observed. At the cellular level, it is postulated that clofarabine triphosphate has multiple mechanisms of action:

1.) Inhibition of DNA polymerase α;

2.) Inhibition of ribonucleotide reductase; and

3.) Disruption of mitochondrial function through release of cytochrome c and pro-apoptotic proteins.

The additive effect of these parallel events leads to the depletion of intracellular deoxynucleotide triphosphate pools, inhibition of elongation of DNA strands during synthesis, and release of pro-apoptotic mitochondrial factors in both actively dividing and quiescent tumor cells, leading to programmed cell death (Parker et al., 1991; Xie and Plunkett, 1996).

Previous studies in adults have shown clofarabine activity in both solid tumors and hematologic malignancies. Kantarjian et al. (2003a) administered clofarabine by 1-hour intravenous infusion once daily for 5 days in a Phase I dose-escalation study. The maximum tolerated dose (MTD) in adult patients with solid tumors was 2 mg/m^2 with the dose-limiting toxicity (DLT) being myelosuppression. In patients with acute leukemias, the MTD was 40 mg/m^2 with the DLT being hepatotoxicty. In 32 patients with acute leukemias, two achieved a complete response and three had a complete response without platelet recovery for an overall response rate of 16%. Later, in a Phase II study in 62 adult patients with acute refractory or relapsed leukemia treated at a daily ×5 dose of 40 mg/m^2, clofarabine had an overall response rate of 48% with the major adverse events being transient liver dysfunction, skin rashes, palmoplantar erythrodyesthesia, and mucositis (Kantarjian et al., 2003b). Clofarabine was also active in the treatment of pediatric patients with advanced leukemias. Jeha et al. (2004) studied the safety and efficacy of clofarabine in 25 pediatric patients, 1 to 19 years old, with relapsed or

refractory leukemia in a Phase I dose-escalation study. Clofarabine was administered daily ×5 for 1 hour at 11.25 to 70 mg/m^2. The MTD was 52 mg/m^2 with the DLT being reversible hepatotoxicity and skin rash. The overall response rate was 32%.

The purpose of this study was to characterize the absorption, distribution, metabolism, and elimination of clofarabine in male, Fischer 344 rats at two target doses, 25 and 50 mg/kg/day for 5 days, and to further examine the *in vitro* metabolism of clofarabine by rat, dog, and human hepatocytes. The strain and doses used in this study were consistent with those used in the GLP-toxicology studies to support clinical development.

Materials and Methods

Chemicals and Reagents. Clofarabine (2-Chloro-9-(2'-deoxy-2'-fluoro-β-D-arabinofuranosyl) 9H-purin-6-amine), 14C-clofarabine, 2-chloroadenine, 2-chloro-9-(2'-deoxy-2'-fluoro-β-D-arabinofuranosyl)-9H-purin-6-one, 6-ketoclofarabine, and clofarabine phosphate were supplied by Genzyme Oncology (San Antonio, TX). The specific activity of 14C-clofarabine was 50.1 mCi/mmol with a radiochemical purity > 98% as determined by HPLC coupled to a radioactivity detector and chemical purity > 99.3% as determined by HPLC and ultraviolet detection. Cryopreserved rat, dog, and human hepatocytes and hepatocyte isolation kits were purchased from XenoTech LLC (Lenexa, Kansas). Hepatocyte incubation media was purchased from In Vitro Technologies (Baltimore, MD). All chemicals were of reagent grade or better.

Animals. Male, Fisher 344 rats (F344/NHsd) approximately 9 to 11 weeks old were obtained from Charles River (Wilmington, MA) and quarantined for 1 week before dosing. Rats were kept in metabolism cages under a 12 hour light:dark cycle maintained at 22 ± 4°C and 50 ± 15% humidity. Rats were allowed food and water *ad libitum* except overnight prior to the Day 5 dose where food was withheld until 4 hours post-dose.

Formulation. Clofarabine and 14C-clofarabine were weighed and transferred into a glass container. PEG 400 was added and the material was stirred until the test article was completely dissolved. The solution was diluted to the final volume using isotonic saline such that the final volume was 25% v/v PEG-400 in 0.9% sodium

chloride. All solutions were stored at approximately ~4°C. A single stock solution was prepared for 5 days dosing. On each day of dosing the required volume was removed from the stock solution and sterilized through a 0.2 μm syringe filter under aseptic conditions. Solutions were equilibrated to room temperature prior to administration. Two stock solutions were prepared, 2.5 and 5.0 mg/mL, to allow dose volumes of ~2.5 mL to be pushed over the dosing interval.

Dose Administration. Each animal was cannulated via the femoral vein at least 1 week prior to the first dose. Each day rats received a slow-push (~3 min) intravenous dose of either 25 or 50 mg/kg 14C-clofarabine (~19 μCi/day, 10 mL/kg). Mass balance doses were administered by weight while doses to determine the plasma concentration time profile were administered by volume. After dose administration, a small volume of heparinized saline was injected into the cannula to maintain patency.

Sample Collection. Pharmacokinetic study. Rats (2/time period/dose group) were anaesthetized with isoflurane at 0, 0.5, 1, 2, 3, 4, 6, 8, 12, and 24 hours post-dose on Day 5 and whole blood was collected by cardiac puncture or from the abdominal aorta. Because of unscheduled deaths in the 50 mg/kg dose group, sample times deviated from the nominal times. Heparinized blood was centrifuged at 5° C and plasma was harvested for radioanalysis and radiochromatographic profiling.

Mass balance. Urine was collected daily during the 5 day treatment period and for three days after the final dose. Urine and feces were collected frozen in glass receivers embedded in dry ice and then daily thawed and processed for radioactivity. The remainder was stored at -20°C for further analysis. After each collection, metabolism cages were rinsed with water and at the end of the mass balance study were washed with detergent and wiped with gauze pads. Rinse volumes were collected and stored frozen for analysis. Carcasses from the mass balance study were frozen and stored for analysis. Due to unexpected deaths, mass balance was not determined in the 50 mg/kg dose group.

Liver and Heart Analyses. The myocardium and liver were collected from rats at 2, 8, and 24 hours after the last dose, were flushed with saline, and stored frozen at -20°C until analyzed. Only those samples in the 50 mg/kg dose group were profiled for

metabolites because samples in the 25 mg/kg dose group had too little radioactivity for analysis.

Quantitative whole body autoradiography (QWBA). In the QWBA study rats received only 25 mg/kg; no 50 mg/kg dose group was studied. Rats (2 per time point) were sacrificed at pre-dose, 0.5, 2, 6, and 30 hours after the last dose on Day 5. Rats were anaesthetized with isoflurane and sacrificed by immediate immersion in a hexane dry ice bath. Carcasses were then placed on dry ice for 2 hours, stored at –70°C, removed from cold storage, and embedded in carboxymethylcellulose together with 14C radioactivity standards used for section thickness quality control. Samples were stored as a carboxymethylcellulose block at –20°C until they were sectioned.

Quantitative Radiochemical Analysis. Plasma, urine, cage wash, and cage rinse. Duplicate aliquots (0.2 mL for plasma and urine and 0.5 mL for cage rinse and cage wash) were transferred to tared scintillation vials and weighed. Ultima Gold (Packard Instruments, Meriden, CT) scintillant (~7 mL) was added to each vial and counted for radioactivity. All samples were counted for radioactivity using a Beckman LS-6000LL liquid scintillation counter. Quench correction was made by the external standard method.

Feces, tissue, and carcass. Feces, myocardium, and liver were thawed and homogenized in three volumes of water (25% w/v). Whole carcasses (including skin) were digested for several days in 5 M potassium hydroxide and methanol (50:50 v/v). The digested carcasses were homogenized with a Tekmar homogenizer. Duplicate homogenate aliquots (~0.5 g for feces and tissues and ~0.2 g for carcass) were transferred to tared cellulose cups and weighed. Carcass cups were neutralized with concentrated hydrochloric acid (~50 µL). Samples were air dried overnight in a hood and then combusted in a sample oxidizer. Approximately 10 mL Carbo-Sorb®E CO_2 absorber (Packard Instruments) and 10 mL Permafluor® E^+ scintillant (Packard Instruments) were added to each vial and counted for radioactivity. All samples were counted for radioactivity using a Beckman LS-6000LL liquid scintillation counter.

QWBA Sample Preparation. Samples were microtomed by a Leica CM 3600 cryo-microtome maintained at -18°C. 40 µm sections were collected at 5 sagittal planes.

The sections were dried in the cryo-microtome chamber and a representative section from each plane, together with 14C autoradiographic standards for subsequent calibration and image analysis, mounted on an aluminum support, wrapped tightly with Mylar film, and exposed to Molecular Dynamics Phosphorimaging screens. The exposed screens were scanned with a Molecular Dynamics Storm 820. The autoradiographic standard image data, generated using American Radiolabeled Chemicals ARC 146 standards, were captured with Imaging Research Inc. AIS software to create a calibrated standard curve. Specific tissue concentrations were determined from interpolation of a standard curve.

Pharmacokinetic Analysis. Pharmacokinetic parameters were determined in the 25 mg/kg dose group by compartmental analysis using WinNonlin Pro (Version 4, Pharsight Corp., Mountain View, CA). A 2- and 3-compartment model was fit to the mean clofarabine radiokinetic profile (expressed as μg-equiv/mL) using inverse concentration as the weights. Clofarabine concentration was calculated based on the total radiokinetic profile that was determined to be parent clofarabine based on metabolic profiling. Model selection was based on the smallest Akaike Information Criteria. Area under the curve was estimated using the linear trapezoidal rule.

Metabolite Profiling and 14C-LC-MS/MS. Rat urine was aliquoted, centrifuged to remove any particulates, and transferred to a clean tube. The supernatant was injected on-column. Plasma from two rats at the same time point were pooled, precipitated and extracted into 9 mL 2% acetic acid in acetonitrile, vortexed for 30 minutes, and centrifuged. The supernatant was transferred to a clean tube, dried under nitrogen at 40°C in a TurboVap, and reconstituted in 300 μL of 10% acetonitrile in mobile phase. The reconstitute was vortexed for 30 minutes, centrifuged, transferred to an HPLC vial, and the supernatant injected on-column.

Rat fecal homogenates (2 mL) from the 25 mg/kg dose group were extracted into 3 mL acetronitrile:water (50:50, v/v) and sonicated for 30 minutes followed by 30 minutes of vortexing. Samples were centrifuged and the supernatant collected into a test tube. The remaining precipitant was then extracted, sonicated, vortexed, centrifuged, and the supernatant collected and pooled with the first supernatant sample. The supernatant was dried in a SpeedVac overnight and reconstituted with 10% acetonitrile in

mobile phase. The reconstitute was sonicated for 20 minutes, centrifuged, transferred to an HPLC vial, and the supernatant injected on-column.

Rat myocardium homogenates collected at the same time point were pooled. Rat myocardium and liver homogenates (2 mL) were precipitated and extracted into 6 mL (9 mL for heart) 2% acetic acid in acetonitrile. Samples were vortexed for 30 minutes, centrifuged, and transferred to a clean tube. Samples were dried overnight under nitrogen at 40°C using a TurboVap. The residue was reconstituted with 50 µL acetonitrile and 50 µL mobile phase. Samples were briefly vortexed, sonicated, transferred to a clean tube, centrifuged, and then transferred to an HPLC vial.

Metabolite profiling and characterization were performed using a radio-LC-MS/MS system consisting of a Sciex API 3000 (Applied Biosystems, Foster City, CA) triple quadrupole tandem mass spectrometer utilizing the ion spray interface in negative mode. The HPLC system interfaced with the mass spectrometer consisted of two Perkin Elmer Series 200 micro LC pumps, a PerkinElmer Series 200 autosampler and a β-ram radioactivity detector equipped with 200 µL ultra high pressure lithium glass cell (IN/US Systems Inc., Tampa, FL). Separation was performed on a Primesphere C18-HC (5 µ, 4.6 x 250 mm) column with C18 (7 µ, 3.2 x 15 mm) guard column, both of which were connected in-line with the radiodetector and mass spectrometer. The mobile phase, consisting of solvent A (water containing 0.1% formic acid and 0.1% ammonium hydroxide) and solvent B (90% acetonitrile, 10% water and 0.1% formic acid and 0.1% acetonitrile) was used throughout. The flow rate was 1 mL/min (of which ~0.2 mL was injected) and elution was accomplished with 10 min isocratic flow at 5% B and 40-min linear gradient from 5 to 12% B followed by 5-min gradient from 12 to 80% B. The effluent from the radioflow detector was split, approximately 0.2 mL/min to the MS and the remainder to waste. A switch valve was used to direct highly aqueous eluate to waste for the first 3 min. The MS/MS experiments were performed by collision-induced dissociation with N_2 as the target gas, and full scan data were acquired. Multiple components were monitored in one LC-MS/MS experiment by separating the total acquisition time in segments, during which MS/MS data were acquired for specific ions.

Radioactivity profiles in plasma and tissue samples were monitored using a radio-LC system consisting of liquid chromatography with accurate radioisotope counting (LC-ARC system). The column was a Primesphere C18-HC (5 μm, 4.6 x 250 mm) kept at 40°C with a C18 guard column (7 μm, 3.2 x 15 mm). The flow rate was 1.0 mL/min with a total run time of 55 minutes. A Packard Radiomatic 150 radioactivity detector was used post-column with a 2.5:1 Stop-Flo AQ scintillant to mobile phase ratio. Counting was done in 20 second fractions with 2 minutes counting time each fraction. The gradient system used was the same as the radio-LC-MS/MS system. This system was not in-line with the mass spectrometer.

Mass Characterization. Mass analyses by LC-MS in the negative ion mode were performed on urine, fecal, plasma, heart, and liver extracts. Characterization of metabolites was conducted using the following approach: full scan mass spectra were generated over the regions where radioactivity was present. The spectra were compared to control samples and then collision-induced dissociation (CID) MS/MS spectra were generated from the unique ions. When CID mass spectra could not be obtained, selective mass transitions were monitored (MRM analysis) corresponding to unique fragment *m/z* 168 (2-chloroadenine). Note: the dosing solution of the *in vivo* study was predominantly parent clofarabine (47:1). LC-MS data were evaluated for the corresponding non-radiolabeled ions.

Metabolism of 14C-Clofarabine in Hepatocytes. The *in vitro* metabolism of 14C-clofarabine in rat, dog, and human hepatocytes was evaluated at 0, 2, and 6 hours using 10 μM 14C-clofarabine incubated at 37° C. Cryopreserved cells were thawed and poured into a Percoll® solution diluted with Dubecco's Modified Eagle Medium (DMEM). The sample was mixed, centrifuged and the dead cell debris was removed. The cells were resuspended in supplemented DMEM solution and centrifuged. The supernatant was discarded and the cells were resuspended in 6 mL of pre-gassed (95% O_2/5% CO_2) incubation media. Viability was determined using trypan blue exclusion. Incubations with 14C-clofarabine were performed in a 6-well plate using an incubation volume of 2 mL per well. Each well received 1 mL of diluted cells (approximately 2 x 10^6 live cells) and 1 mL of a 20-μM solution of 14C-clofarabine. Incubations were

terminated at 2 and 6 hours by the addition of 4 mL of 2% acetic acid in acetonitrile. Negative controls were prepared with heat deactivated cells (80°C for 5 min). Positive controls were prepared by spiking the cells with 10 μM dextromethorphan, 5 μM midazolam, and 25 μM 7-hydroxycoumarin.

Preparation of Samples for Mass Spectral Analysis. Hepatocyte samples were centrifuged at 3,000 rpm for 10 min. The supernatant was evaporated to dryness under N_2 and the residue was resuspended in 250 μL of 20% acetonitrile/H_2O for subsequent analysis by an LC-MS/MS coupled to a radioactivity detector. Urine samples (1 mL) were clarified by centrifugation at 12,000 rpm for 5 min. The resulting supernatants were analyzed by LC-MS/MS coupled to a radioactivity detector. Equal volumes of plasma (1.5 mL) were combined for each selected time point. Preweighed myocardium and liver samples were homogenized in ~3 volumes of deionized water. The proteins from each matrix were precipitated with 3 volumes of acetonitrile containing 2% acetic acid. After centrifugation at 3,500 rpm for 10 min, the supernatant was evaporated to dryness under N_2 and the residue was resuspended in 300 μL of 10% acetonitrile/mobile phase A for subsequent analysis by LC-MS/MS coupled to a radioactivity detector. Weighed fecal samples were homogenized with ~3 volumes of deionized water. Each homogenate (~2 g) was extracted twice with 3 mL of 50% acetonitrile/water. The two organic extracts were combined and evaporated to dryness in a vacuum evaporator overnight. The residue was resuspended with 200 μL of 10% acetonitrile/mobile phase A, sonicated, vortexed and centrifuged at 12,000 rpm for 5 min. The clear supernatant was analyzed by LC-MS/MS coupled to a radioactivity detector.

Results

C**linical Observations**. Rats given the 25 mg/kg/d 3 minute infusion exhibited transient labored breathing and sedation. All rats given the 50 mg/kg/d regimen died after 1 – 3 days of dosing. Clinical signs preceding death included labored breathing, reddish-brown liquid around the nose and mouth, and bluish skin color. Blood, myocardium, and liver samples were collected as soon as possible following death and concentrations of radioactivity quantitated.

Pharmacokinetic Results in the 25 mg/kg Dose Group. Mean trough concentrations of radioactivity in plasma at steady-state were low (< 0.1 µg-equiv/g). Total radioactivity expressed as a parent concentration based on metabolic profiling was best described by a 3-compartment model with α-, β-, and γ-half-lives of 0.3, 1.3, and 12.8 hours, respectively (Figure 2). The final parameter estimates (± SE) were 1264 ± 57 mL/h/kg for clearance, 1.1 ± 0.18 L/kg for the central volume of distribution, 829 ± 85 mL/kg for the volume of the peripheral compartment, 934 ± 151 mL/h/kg for intercompartmental clearance to the peripheral compartment, 2.9 ± 2.1 L/kg for the volume of the deep compartment, 182 ± 40 mL/h/kg for intercompartmental clearance to the deep compartment, and 4.9 ± 2.2 L/kg for the volume of distribution at steady-state. The volume of the deep compartment was not estimated with the same degree of precision as other model parameters, but inclusion of the deep compartment was necessary to adequately characterize the data.

Mass Balance and Profiling in the 25 mg/kg Dose Group. Mean trough concentrations of radioactivity in liver and myocardium at steady-state were 8 to 9-fold higher than plasma (0.8 and 0.9 µg-equiv/g, respectively). Concentrations of radioactivity in liver averaged 16.1, 2.2, and 0.8 µg-equiv/g at 2, 8, and 24 hours post-dose, respectively. Tissue:plasma ratios for radioactivity in liver averaged 6.3, 10.9, and 11.3 at 2, 8, and 24 hours post-dose, respectively. Concentrations of radioactivity in myocardium averaged 12.3, 3.5, and 0.9 µg-equiv/g at 2, 8, and 24 hours post-dose, respectively. Tissue:plasma ratios for radioactivity in myocardium averaged 4.8, 16.7, and 12.8 at 2, 8, and 24 hours post-dose, respectively.

Radioactivity recoveries 0 to 24 hours after the fifth dose averaged 77.1 ± 3.1% in urine and 10.8 ± 0.6% in feces. An additional 6.0 ± 2.7% of the radioactive dose was recovered in cage wash. Less than 1% of the dose was recovered in carcass. The total mass balance recovery, determined for 3 days after the final (Day 5) dose, was 95.3 ± 0.5%. A total of 87.2% of the radioactivity in urine excreted 0-24 hours after the last dose could be attributed to unchanged clofarabine. If cage wash radioactivity is assumed to represent primarily urinary radioactivity (which is a reasonable assumption because no significant fecal contamination was evident in cage wash), then 72.4% of the

administered dose was excreted in urine as unchanged clofarabine and 10.6% of the dose was excreted in urine as metabolites. Similarly, 10.8% of the administered dose was recovered in feces on Day 5.

Metabolic profiling results indicated that about 6.9% of the radioactivity in feces was unchanged clofarabine. Therefore, approximately 0.75% of the dose was eliminated in feces as unchanged clofarabine and 10.1% of the dose was eliminated in feces as metabolites. If these values (based on the observed mean recovery of 95.3% of the dose) are scaled to 100%, approximately 76.0% of the 25 mg/kg dose was excreted in urine as unchanged clofarabine, 21.7% was eliminated in urine and feces as metabolites, and 0.8% was eliminated as unchanged clofarabine by either biliary secretion, colonic secretion, or hydrolysis of glucuronide conjugates in the gut. Clofarabine metabolites were eliminated in approximately equal fractions by renal clearance (51%) and biliary clearance (49%). The total amount of administered dose recovered in urine as unchanged clofarabine and metabolites was 4.7 mg and the $AUC_{0–24}$ of radioactivity was 17.1 µg-equiv*h/g. Therefore, the total estimated renal clearance of radioactivity was 275 mL/h. Because 87.2% of the radioactivity in urine represented unchanged clofarabine, the estimated renal clearance of clofarabine was 240 mL/h.

Pharmacokinetic Results in the 50 mg/kg Dose Group. Because of the unscheduled deaths after 1 to 3 doses of this regimen, it was not possible to characterize the concentration versus time profile of radioactivity. Blood samples were collected as soon as possible following death for quantification of plasma radioactivity concentrations. Actual sample collection times from treated animals at the time of death ranged from mid-infusion to 3 hours post-dose, with most samples collected at or near the end of the 3-min infusion. Because samples could not be obtained at the nominal times after the 50-mg/kg dose, it was not possible to directly compare radioactivity concentrations between the 25- and 50-mg/kg dose groups. Therefore, linearity was assessed by compartmental modeling. Based on a 3-compartment model following intravenous infusion of 25-mg/kg dose, the estimated maximum plasma concentration at the end of a slow bolus would be 20.4 µg-equiv/g. Assuming linear pharmacokinetics, after a slow bolus of 50-mg/kg the estimated plasma radioactivity concentration would be 40.8 µg-equiv/g. The observed concentration at 0.05 hours after the 50-mg/kg dose was

120 µg-equiv/g, which was ~3-fold higher than expected. Similarly, the theoretical concentration for a 50-mg/kg dose was 28 µg-equiv/g at 0.25 hours post-dose, but the observed mean concentration was 50.8 µg-equiv/g, or ~2-fold higher than expected. These differences exceed the anticipated range of variability from experimental error and suggest nonlinear pharmacokinetics between 25- and 50-mg/kg.

Metabolite Profiling in the 25 mg/kg Dose Group. The counting efficiency of the radio-LC-MS/MS system ranged from 30 to 43% with a counting efficiency of < 10%. The mean recovery after injecting urine and fecal extracts on-column was 100%. The LC-ARC system had a counting efficiency of 60 to 96% with a counting precision of 6 to 21%. The extraction recoveries of fecal, plasma, and tissue homogenates ranged from 89% to 115%.

Based on region of integration (ROI), instead of daily recovery of radioactivity (DRR), six metabolites were observed in plasma (Table 1). Clofarabine accounted for 63% (24 hours post-dose) to 93% (0.5% post-dose) of the ROI. Of the metabolites, P9a (which was later identified and confirmed as 6-ketoclofarabine) accounted for 4% of the ROI at 0.5 hours post-dose but was 37% of the ROI 24 hours post-dose (Table 2). The ratio of P9a to clofarabine increased over time.

The peak numbering system of the radiochromatograms incorporated all peaks observed in all the *in vitro* and *in vivo* matrices evaluated (Figure 3). Overall, radiochromatograms were divided into 17 radioactivity regions, each of which may contain one or more metabolites. Region P6 and P10 were observed exclusively in the *in vitro* hepatocyte study. Eight metabolite peaks were observed in urine, of which clofarabine (P15) accounted for 68 to 74% of the DRR. The next most abundant peaks were P9a (7% DRR), P8 (1.5% DRR) and P13 (1.5% DRR). The minor metabolites accounted for less than 0.7% of the DRR. Thirteen (13) peaks were observed in feces, which accounted for ~0.7% of the DRR. The major metabolite observed was P9a, which accounted for 7% of the DRR, followed by P14 (1.7% of the DRR), with the remainder accounting for less than 0.9% of the DRR.

Concentrations and Metabolite Profiling of Plasma, Myocardium, and Liver in the 50 mg/kg Dose Group. No excreta were analyzed in the 50 mg/kg dose group due

to premature deaths. Because of unscheduled deaths, concentrations of radioactivity in liver and myocardium could not be determined at the nominal sampling times. Radioactivity concentrations in liver averaged 144 µg-equiv/g immediately after the third dose and 135 µg-equiv/g at 0.25 hours after the third dose. Corresponding concentrations of radioactivity in myocardium averaged 125 and 91.0 µg-equiv/g. Tissue:plasma ratios were not calculated because the data were not from Day 1 and concentrations were not at steady-state. Therefore, tissue:plasma ratios could not be compared between the 25- and 50-mg/kg doses.

In those plasma samples collected immediately after death, clofarabine accounted for more than 91% of the ROI in most animals. One animal survived to 3 hours post-dose on the third day. In that animal, six plasma metabolites were observed, of which clofarabine accounted for 77% of the ROI, followed by P12 (10% ROI), and P9a (6.5% ROI). The remaining metabolites accounted for less than 2% of the ROI. In myocardium and liver radiochromatograms, parent clofarabine accounted for 94% to 99% of the ROI. Five metabolites were observed in myocardium, while seven were observed in the liver. The major metabolite in heart and liver was P9a, which accounted for < 2% of the ROI.

Mass Characterization. Table 3 presents the parent ions and major fragment ions of clofarabine and authentic reference metabolites following LC-MS/MS analyses under negative mode of detection. Figure 1 presents the postulated metabolites of clofarabine across the *in vivo* and *in vitro* studies. In the mass spectrum of clofarabine (P15, MW 303 Da, $(M-H)^-$ = 302), the largest ion in the mass spectrum at *m/z* 348 corresponds to the formic acid adduct of the parent drug and an artifact of the ammonium formate buffer used in the LC mobile phase. The CID spectra of *m/z* 302 with the characteristic fragments *m/z* 282, 264, 246, 234, 224, 168 and 132. CID analysis of *m/z* 348 showed fragment ions *m/z* 302, 282, 246, 224 and 168 (data not shown).

The molecular ion for P7 was *m/z* 168, which corresponds to the N-dealkylation of the furanosyl moiety to yield 2-chloroadenine. CID analysis of *m/z* 168 in P7 was congruent with that of the 2-chloroadenine standard (data not shown). P7 was only observed in fecal samples.

The molecular ion for P9a was *m/z* 303, which corresponds to the addition of 1 amu to clofarabine. The most likely change to account for this mass difference is the displacement of the 6-amino group (NH_2, 16 amu) of the adenosyl moiety by a hydroxyl group (OH, 17 amu). CID analysis of *m/z* 303 showed similar fragmentation pattern as clofarabine, with 1 unit mass shifts for each of the fragment ions. CID spectrum of P9a was congruent with the CID spectrum of 2-chloro-9-(2'-deoxy-2'-fluoro-β-D-arabinofuranosyl)-9H-purin-6-one standard. The metabolite was subsequently renamed 6-ketoclofarabine. P9a was observed in every matrix.

The molecular ion for P11 was *m/z* 316, which corresponds to an addition of 14 Daltons indicating the presence of a double-bonded oxygen or methylation. The most likely site for the addition of the double-bonded oxygen is at the 5' carbon of the furanosyl moiety, changing the alcohol to an acid; methylation could occur at either of the furanosyl -OH groups. CID analysis of this peak showed primarily the characteristic fragment ion *m/z* 168 indicating the adenine part of the molecule is unmodified. The exact location of the change and whether it corresponds to methylation or oxidation is unknown. P11 was observed in urine, feces, and plasma.

The molecular ion for P12 and P13 was *m/z* 480, resulting from the addition of 176 Daltons and corresponds to the glucuronide of clofarabine. Due to low intensity, no fragmentation of the *m/z* 480 was observed in CID mass spectra. The presence of the characteristic fragment ions *m/z* 304, 226 and 170 in the MRM analysis verifies that *m/z* 480 is a metabolite of clofarabine. The possible site for the addition of glucuronide is on the oxygen at the 3' or 5' carbon. Although *m/z* 480 was not observed in the MS spectra of human hepatocyte samples, MRM analysis indicated its presence. Clofarabine glucuronides were not observed in rat samples, but only in the *in vitro* hepatocyte study.

The molecular ion for P13 (urine) and P14 (feces) was also *m/z* 382. The addition of 80 Daltons would correspond to either the phosphate or sulfate conjugate of clofarabine. However, CID analysis of the *m/z* 382 peak from urine or feces did not show the presence of characteristic phosphate fragment ion *m/z* 79. The chromatographic separation (different retention times) of P13 and P14 indicates the presence of two

isomers of the sulfate conjugate. In addition to feces, P14 was also observed in rat plasma and tissues.

Clofarabine phosphate has been reported to be the major metabolite in human T-lymphoblast leukemia CCRF-CEM cells (Xie and Plunkett, 1996). Clofarabine phosphate has weak ionization response and a similar retention time as the hydroxy-clofarabine (*m/z* 303, P9b). The CID spectrum of *m/z* 382 from the clofarabine phosphate standard indicated the presence of *m/z* 168, which is a characteristic fragment ion of the unmodified adenine moiety, and *m/z* 79 of the phosphate ion. Initial evaluation of the electrospray mass spectrum of the urine, feces, plasma, heart, and liver sample matrices did not show the presence of clofarabine phosphate (*m/z* 382). Reanalyses by selectively monitoring the transitions of *m/z* 382 to product ions *m/z* 168 and 79 indicated the possible presence of clofarabine phosphate in the region of P9b in urine, plasma, myocardium, and liver, although these were below the detection limit. Clofarabine phosphate was not observed in feces. Attempts to chromatographically separate the 6-ketoclofarabine and the clofarabine phosphate peaks were unsuccessful and therefore the relative amount of clofarabine phosphate could not be estimated. Moreover, experimentation with spiking clofarabine phosphate to fecal extracts showed the disappearance of the *m/z* 382 response indicating either ion suppression or instability of the compound. Extracted ion chromatogram analyses of the total ion spectra from the biological samples for the clofarabine di-phosphate ion (*m/z* 462) or tri-phosphate ion (*m/z* 542) did not indicate the presence of these metabolites. MRM analyses for these metabolites were not performed.

Mass spectral analysis of the radioactive regions P1-P5, P12, and P16-P17 from the chromatograms of rat urine, feces, plasma, or tissues did not reveal distinguishable ions apart from those seen with control samples. CID analysis of these peaks were therefore not conducted. In total, these peaks represented < 3% of the excreted radioactivity.

Quantitative Whole Body Autoradiography. The limit of quantification (BLQ) was set at 0.274 µg-equiv/g. Distribution of radioactivity to tissues was widespread following the final intravenous dose of 25 mg/kg/day (Figure 4). The distribution of

radioactivity in male rats was widespread at 0.5 hours after the final dose with most tissues reaching their maximal concentration at this point. The highest concentrations of radioactivity were found in the urine and the urinary bladder (440 and 254 µg-equiv/g, respectively). High concentrations of the administered dose were also found in the spleen, kidney, cecum, and thymus (123, 82, 65, and 62 µg-equiv/g, respectively). Most measured tissues had concentrations greater than plasma, i.e., tissue to plasma ratios were larger than one. Distribution of radioactivity in the kidney was relatively homogenous. Biliary excretion could not be confirmed, as radioactivity was not measurable in the bile (within hepatic ducts of the liver). Low concentrations (approximately 13- to 34-fold less than blood) of 14C-clofarabine-derived radioactivity were detected in the tissues of the central nervous system. Distribution of radioactivity in the tissues of the central nervous system was homogenous and showed no evidence of differential localization. Elevated radioactivity concentrations in the lower gastrointestinal (GI) tract were probably the result of continued elimination of drug-derived radioactivity from the previous day's dose. The lowest measurable tissue concentrations of radioactivity were found in the seminal vesicle, cerebellum, cerebrum, spinal cord, and medulla (3, 0.8, 0.6, 0.5, and 0.3 µg-equiv/g, respectively).

By 2 hours after the final dose, the overall distribution of 14C-clofarabine-derived radioactivity in male rats remained widespread, although overall concentrations began to decline. The highest concentration of radioactivity was found in urine (241 µg-equiv/g) and urinary bladder (175 µg-equiv/g). High concentrations of radioactivity were found in the cecum contents, small intestinal contents, and large intestinal contents, indicating transit of the administered dose in the GI tract. The small intestinal wall was the only measured tissue that reached maximal concentrations at 2 hours post-dose. Radioactivity concentrations decreased by 2- to 4-fold in the major organs of excretion (liver and kidney). The spleen, thymus, harderian gland, and lymph nodes (44, 28, 23, and 23 µg-equiv/g, respectively) had concentrations of radioactivity that exceeded the concentrations found in the liver and kidney. Drug–derived radioactivity incorporated into the hair 2 hours after the final dose was 39 µg-equiv/g. The myocardium concentration was 2-fold higher than that found in skeletal muscle and 4-fold greater than the blood concentration. The remainder of the non-GI tract tissues had radioactivity

concentrations that were less than 16 µg-equiv/g. The lowest quantifiable concentrations were found in the preputial gland, spinal cord, and medulla of the brain (< 0.4 µg-equiv/g, respectively) at this sampling time.

At 6 hours post-dose, further declines in 14C-clofarabine-derived radioactivity were found in the majority of tissues, though distribution of radioactivity remained widespread. Excluding the GI tract, the urine and urinary bladder had the highest concentrations of radioactivity (111 and 33 µg-equiv/g, respectively). The large intestinal contents and cecum contents reached the maximum observed concentration at 6 hours after the final dose indicating further elimination of drug-derived radioactivity. Hair (25 µg-equiv/g) was the only other measured matrix that contained more that 5 µg-equiv/g at this time point. The following tissues had radioactivity concentrations that were below the limit of quantification (BLQ): cerebellum, cerebrum, medulla, and spinal cord.

By 30 hours after the final Day 5 dose, overall radioactivity continued to decline as continued elimination of drug-derived radioactivity was evident. Radioactivity concentrations in the spleen, kidney, and liver fell 322-, 212-, and 73-fold, respectively. The majority of the remaining radioactivity was associated with the contents of the GI tract, urine, and hair. The highest concentration value, 23 µg-equiv/g, was found in the hair, followed by the large intestinal contents, urine, cecum contents, and urinary bladder (18, 13, 11, and 5 µg-equiv/g, respectively). All other measured matrices had concentrations lower than 1.5 µg-equiv/g. Twenty-three of 53 measured tissues were BLQ by 30 hours after the final Day 5 dose. Elimination of drug-derived radioactivity was not complete at the final sampling time.

In summary, high radioactivity was present in urine and kidney suggesting rapid renal excretion of drug-derived radioactivity. The majority of tissues reached maximum concentrations at 0.5 hour post-dose and then declined steadily over time. Although distribution was fairly homogeneous, decreased radioactivity was observed in tissues with special barriers compared to other tissues at all time points. The distribution of radioactivity in the tissues of the central nervous system was uniform with no evidence of differential distribution. Hence, the highest postdistributive concentrations of

radioactivity were in the excretory organs, kidney, bladder and GI tract, with no remarkable suborgan distribution.

In vitro hepatocyte metabolism. The appearance of the appropriate Phase I and II metabolites in the positive controls, and the absence of metabolites in the negative control, indicated that the system was acting appropriately. Metabolism of clofarabine in rat, dog, and human hepatocytes was minimal following 6 hours incubation of 10 μM 14C-clofarabine. The percent of clofarabine remaining ranged from 95 to 98.8% (Table 4). In rat and dog hepatocytes, the major metabolite observed was P11 accounting for 1.2 and 2.5% of the radioactivity in the chromatogram, respectively. P11 is proposed to be a carboxy- or methoxy-clofarabine. The only metabolite observed in human hepatocytes was P14, which is proposed to be the sulfate conjugate of clofarabine and accounted for 0.2 % of the radioactivity in the chromatogram.

Discussion

The results of this study indicate that clofarabine exhibited nonlinear pharmacokinetics at the doses examined: 25 and 50 mg/kg daily for 5 days. Qian et al. (1994) suggested that clofarabine has nonlinear pharmacokinetics after single dose intravenous and oral administration of 10 and 25 mg/kg. The results from this study corroborated their observation. In the GLP toxicology studies, clofarabine administration in rats induced adverse histopathological effects on the heart at 50 mg/kg/day after 5 days treatment and at 25 mg/kg/day for 5 days after 6 cycles of treatment, but was not observed at lower doses (internal data). Nonlinear pharmacokinetics may be playing a role in the degree of toxicity as it has been observed that prolonging the infusion length and changing the route of administration from intravenous to oral (which also blunts maximal concentrations) reduces the degree of cardiotoxicity. Further, such cardiotoxicity has only been seen in rats and may be species-dependent. In this study, the maximal clofarabine concentration after intravenous bolus administration of 25 and 50 mg/kg was ~20 and 120 μg/mL, respectively, the latter being a predicted value. In the Phase II human studies in pediatric and adult patients with leukemia the recommended doses are 52 mg/m^2 and 40 mg/m^2, respectively, given by 1 to 2 hour infusion. At these doses, the observed maximal concentrations ranged from 0.14 to 1.05 μg/mL in pediatric

patients and from 0.24 to 1.92 μg/mL in adults. Hence, these data suggest a more than 15-fold safety margin between animals and humans.

At steady-state, tissue distribution of radioactivity based on QWBA was widespread and showed highest concentrations in the rapidly perfused tissues. Radioactivity distribution was widespread with the highest concentrations observed in the excretory organs, i.e., gastrointestinal tract and kidneys. No tissue showed selective accumulation and only tissues with special barriers showed restrictive distribution. Previous studies in mice have shown that the distribution of nucleoside analogs, clofarabine included, is uniform and rapid with the highest concentrations found in the rapidly perfused tissues (Lindemalm et al., 1999). Low plasma protein binding has been reported for clofarabine in rats (13%, Qian et al., 1994) and humans (47%, Reichelova et al., 1995) indicating that a large fraction of the compound circulating in blood is present in the free form and available for cellular uptake. This difference in protein binding may also help explain the greater toxicity in the rat than in humans since more unbound drug is available for tissue distribution in rats than humans. Further, clofarabine has low lipophilicity with a mLogP of -0.17 indicating almost equal preference for water and lipid. With a large fraction of drug available for distribution and low lipophilicity, it was expected that distribution in the rat would not favor particular tissues, unless that tissue had a specific nucleoside transporter (which did not appear to be the case).

The major metabolite formed was 6-ketoclofarabine, which was found in all matrices examined, but accounted for less than 10% of the radioactivity in all the tissues examined. Interestingly, clofarabine was metabolically stable in isolated hepatocytes, having more than 95% remaining intact after 6 hours incubation in all three species, indicating that clofarabine does not undergo CYP metabolism to any significant extent and that the location of the enzyme responsible for its metabolism to 6-ketoclofarabine is extra-hepatic. The identity of the enzyme responsible for metabolism of clofarabine to 6-ketoclofarabine is unknown, but given the close structural similarity of clofarabine to adenosine, a likely possible enzyme is adenosine deaminase, an ubiquitous enzyme of purine metabolism that catalyzes the irreversible deamination of adenosine and

deoxyadenosine to inosine and deoxyinosine, respectively. Further studies are needed to confirm this hypothesis.

References

Jeha S, Gandhi V, Chan KW, McDonald L, Ramirez I, Madden R, Rytting M, Brandt M, Keating M, Plunkett W, Kantarjian H. Clofarabine, a novel nucleoside analog, is active in pediatric patients with advanced leukemia. Blood 2004; 103; 784-789.

Kantarjian HM, Gandhi V, Kozuch P, Faderl S, Giles F, Cortes J, O'Brien S, Ibrahim N, Khuri F, Du M, Rios MB, Jeha S, McLaughlin P, Plunkett W, Keating M. Phase I clinical and pharmacology study of clofarabine in patients with solid and hematologic cancers. J. Clin. Oncol. 2003a; 21; 1167-1173.

Kantarjian H, Gandhi V, Cortes J, Verstovsek S, Du M, Garcia-Manero G, Giles F, Faderl S, O'Brien S, Jeha S, Davis J, Shaked Z, Craig A, Keating M, Plunkett W, Freireich E. Phase 2 clinical or pharmacologic study of clofarabine in patients with refractory or relapsed acute leukemia. Blood 2003b; 102: 2379-2386.

Lindemalm S, Liliemark J, Larsson BS, Albertioni F. Distribution of 2'-chloro-2'-deoxyadenosine, 2-chloro-2'-arabino-fluoro-2'-deoxyadenosine, fludarabine, and cytarabine in mice: a whole body autoradiography study. *Med Oncology* 1999; 16: 239-44.

Parker WB, Shaddix SC, Chang CH, et al. Effects of 2-chloro-9-(2-deoxy-2-fluoro-□-D-arabinofuranosyl)adenine on K562 cellular metabolism and the inhibition of human ribonucleotide reductase and DNA polymerases by it's 5'-triphosphate. Cancer Research 1991;51:2386-2394

Qian M, Wang X, Shanmuganathan K, Chu CK, Gallo JM. Pharmacokinetics of the anticancer agent 2-chloro-9-(2-deoxy-2-fluoro-β-D-arabinofuranosyl)adenine in rats. *Cancer Chemother Pharmaco.* 1994; 33: 484-8.

Reichelova V, Liliemark J, Albertioni F. Structure-activity relationships of 2-chloro-2'-arabino-fluoro-2'-deoxy-adenosine and related analogues: protein binding, lipophilicity, and retention in reversed phase HPLC. *J Liq Chrom* 18; 1995: 1123-35.

Xie KC, Plunkett W. Deoxynucleotide pool depletion and sustained inhibition of ribonucleotide reductase and DNA synthesis after treatment of human lymphoblastoid cells with 2-chloro-9-(2-deoxy-2-fluoro-β-D-arabinofuranosyl)adenine. *Cancer Research* 1996;56:3030-3037.

Footnotes

Financial Disclosure: All work was sponsored by Genzyme Oncology. PLB and LA are employees of Genzyme Oncology. All other authors have no financial affiliations with Genzyme Oncology.

Legends for Figures

Figure 1: Postulated structures for clofarabine and its metabolites. * denotes placement of 14C-radiolabel.

Figure 2: Plasma concentration-time profiles for clofarabine, total radioactivity, and 6-ketoclofarabine in the 25 mg/kg dose group at steady-state on Day 5. Solid line is the predicted concentration based on a 3-compartment model. Open circles are parent clofarabine concentrations based on metabolite profile.

Figure 3: Sample radiochromatograms from clofarabine standard, urine, feces, plasma, liver, and myocardium. Urine and fecal samples were collected 24 hour post-dose. The plasma, liver, and myocardial samples were collected 0.5, 1, and 1 hour(s) after dosing.

Figure 4: Representative whole body autoradioluminograph of radioactivity taken 0.5 hours post-dose on Day 5 after a 5-day once daily 25 mg/kg/day intravenous dosing regimen of 14C-clofarbine. All sections are from the same animal and represent a lateral saggital (top figure) to mid-saggital (bottom figure) view.

Table 1. Presence of clofarabine and radioactive metabolites in radiochromatograms of rat plasma, tissue and excreta and in rat, dog, and human hepatocytes. Summary of radioactive peak regions observed (marked with X) in the chromatograms of the evaluated matrices from the *in vitro* and *in vivo* studies.

Peak Name	Ret Time (min)	Rat Hepatocytes	Dog Hepatocytes	Human Hepatocytes	Rat Plasma	Rat Tissue	Rat Urine	Rat Feces
P1	2-3				X		X	X
P2	3-4				X			X
P3	4-5				X			X
P4	6-7				X	X		X
P5	8-9				X	X	X	X
P6	12-15		X					
P7	15-17	X	X					X
P8	17-19	X			X	X	X	X
P9	19-23	X	X		X	X	X	X
P10	23-26	X	X					
P11	25-29	X	X		X		X	X
P12	29-30	X	X		X	X		X
P13	30-32	X			X		X	X
P14	32-34	X	X	X		X		X
P15*	36-39	X	X	X	X	X	X	X
P16	37-41	X			X	X	X	X
P17	42-46				X		X	

* denotes that peak is parent clofarabine.

Table 2. Metabolite profile of rat plasma in the 25 mg/kg dose group on Day 5 presented as percent radioactivity in chromatogram (tissue values are in parentheses).

Time (h)	P5	P8	P9	P11	P12	P15 (Parent)	P17
0.5	ND	1.2	3.6	0.7	1.3	93.2	0.1
1	ND	1.5	5.7	0.6	1.1	90.4	0.7
2	ND	1.2	7.9 (heart: 1.4, liver: 0.9)	0.6	1.0	89.3 (heart: 98.6, liver: 96.8)	(liver: 2.2)
3	0.93	1.5	11.9	1.5	ND	84.2	ND
4	ND	2.1	13.3	ND	ND	84.6	ND
6	ND	3.4	19.6	ND	ND	77.0	ND
8	ND	3.2	14.0	ND	ND	82.9	ND
12	ND	ND	32.0	ND	ND	68.0	ND
24	ND	ND	37.0	ND	ND	63.0	ND

ND denotes ‘not detected’.

Table 3. Parent ions and major fragment ions of clofarabine and authentic reference metabolites following LC-MS/MS analyses under negative mode of detection

Peak	Description	$(M^{**}-H)^-$ *m/z*	Major Fragment Ions
1-6	Unknown	NS	NA
7	2-Chloroadenine	168	**132**
8	Unknown (rat)	343	ND
9a	6-Ketoclofarabine	303	**133**, 169, 189, 225, 235, 265, 283
9b	Clofarabine phosphate	382	79, **168**, 195, 213
9c	Unknown (rat)	392	ND
10	Unknown	ND	ND
11	Carboxy- or methoxy-clofarabine	316	132**, 168**, 198
12	Clofarabine-glucuronide (rat and dog)	478	ND
13a	Clofarabine-sulfate	382	**168**, 213, 362
13b	Clofarabine-glucuronide (rat)	478	ND
14	Clofarabine-sulfate (rat, dog, human)	382	**168**, 213, 362
15*	Clofarabine	302	132, **168**, 188, 198, 224, 228, 234, 246, 264, 282
16	Unknown	NS	NA
17	Unknown	NS	NA

* denotes that peak is parent clofarabine.
** denotes non-radiolabeled mass.
In parenthesis are metabolites observed from in vitro hepatocyte studies.
Most intense ions are presented in bold.
NS: not studied.
NA: not applicable.
ND, not detected.

Table 4. Metabolite profiles of rat, dog, and human hepatocyte samples following 10-μM incubation of 14C-clofarabine for 6 hours (% radioactivity in the chromatogram).

Species	P6	P7	P8	P9	P10	P11	P12	P13	P14	P15	P16
Rat	ND	0.4	0.4	0.4	0.7	1.2	0.9	0.1	0.5	95.8	0.2
Dog	0.4	0.5	ND	0.6	ND	2.5	0.8	ND	0.4	94.8	ND
Human	ND	ND	ND	ND	ND	ND	ND	ND	0.2	99.8	ND

ND: not detected.

Figure 1

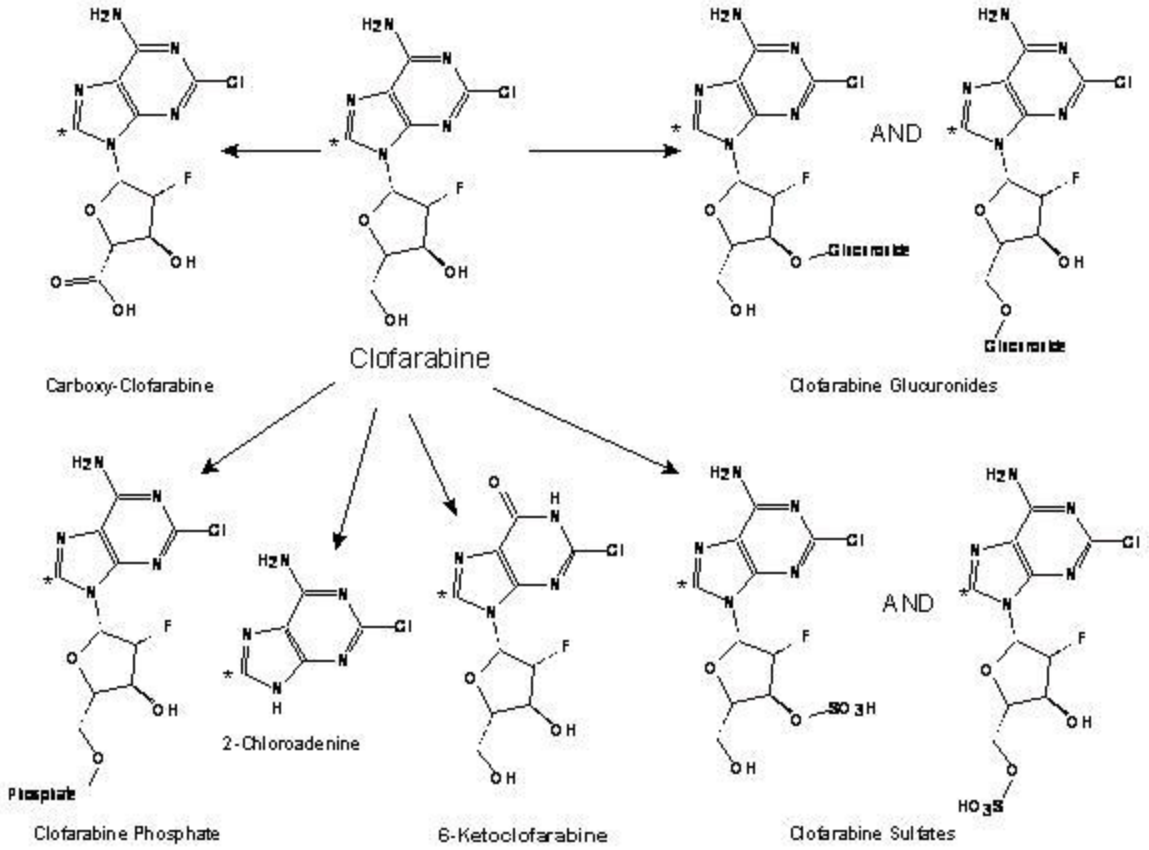
Clofarabine
Carboxy-Clofarabine
Clofarabine Glucuronides
AND
Clofarabine Phosphate
2-Chloroadenine
6-Ketoclofarabine
Clofarabine Sulfates
AND

Figure 2

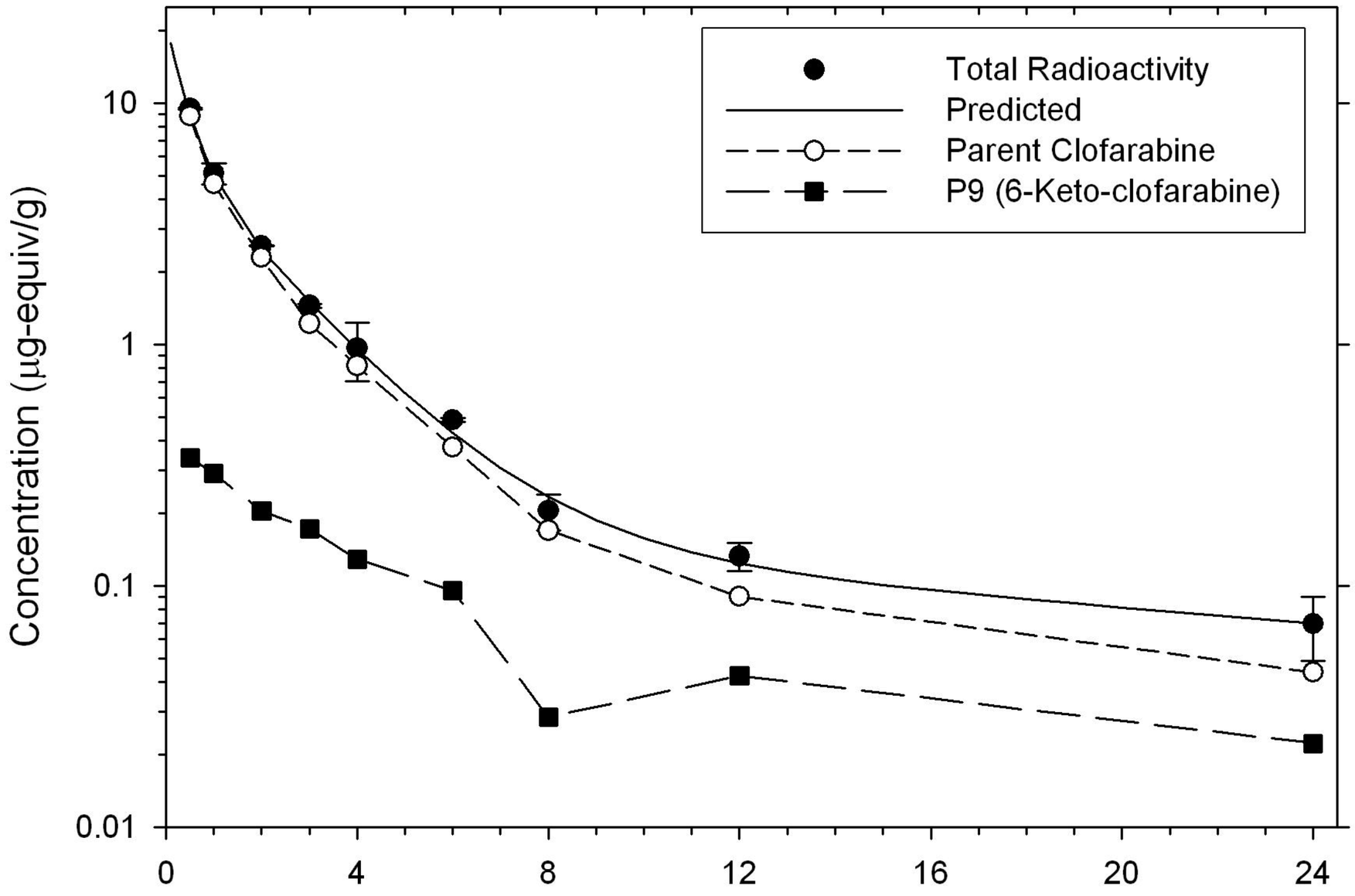
Total Radioactivity
Predicted
Parent Clofarabine
P9 (6-Keto-clofarabine)
Concentration (µg-equiv/g)
10
1
0.1
0.01
0
4
8
12
16
20
24
Time (hours)

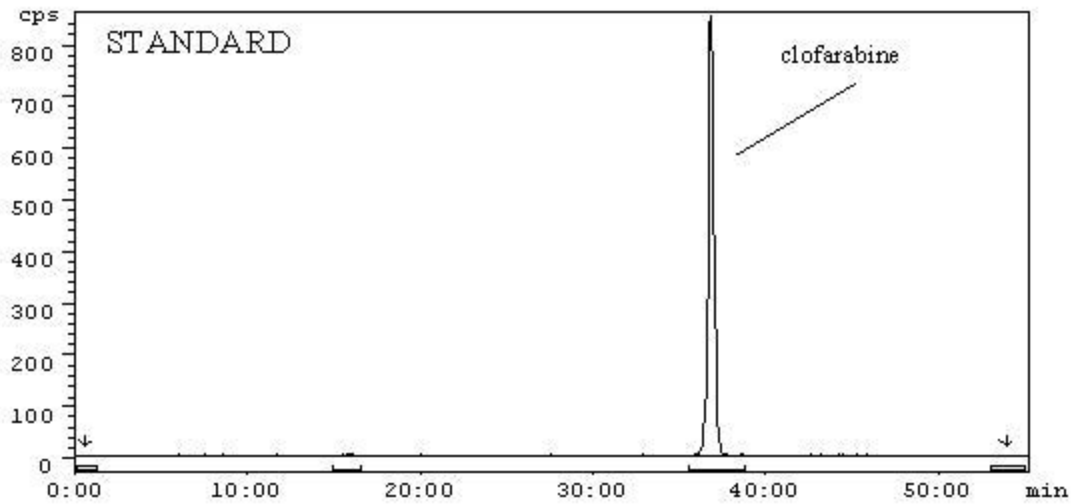

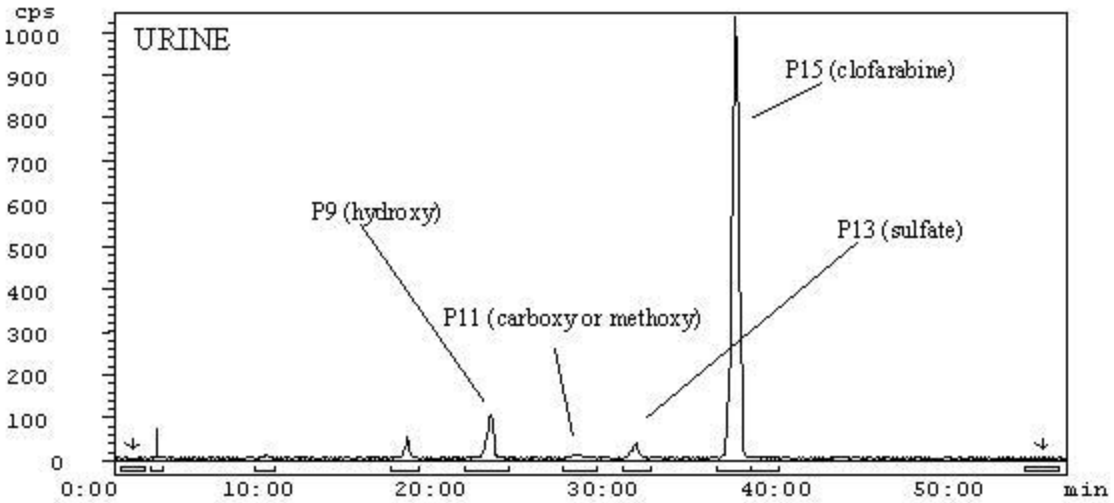

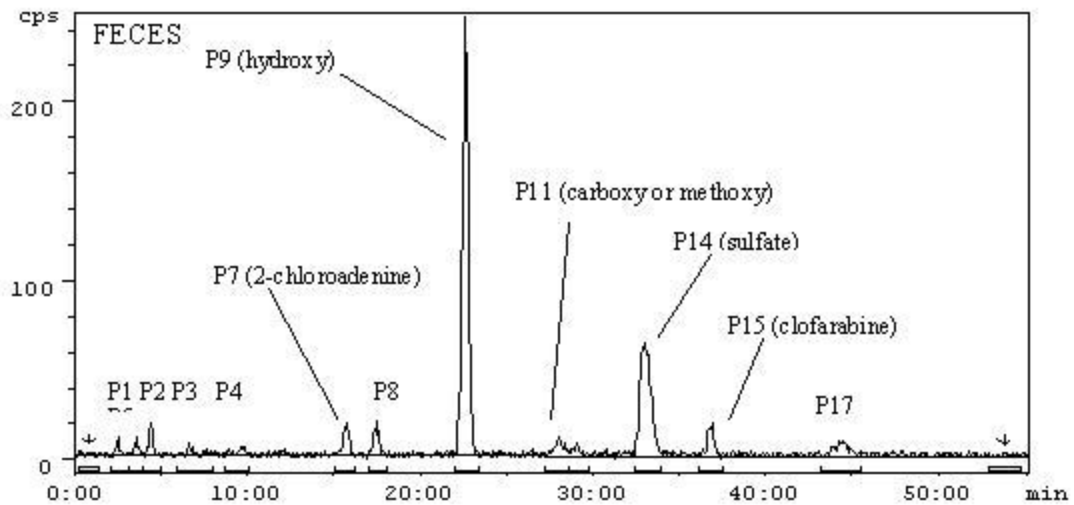

Figure 3 (1 of 2)

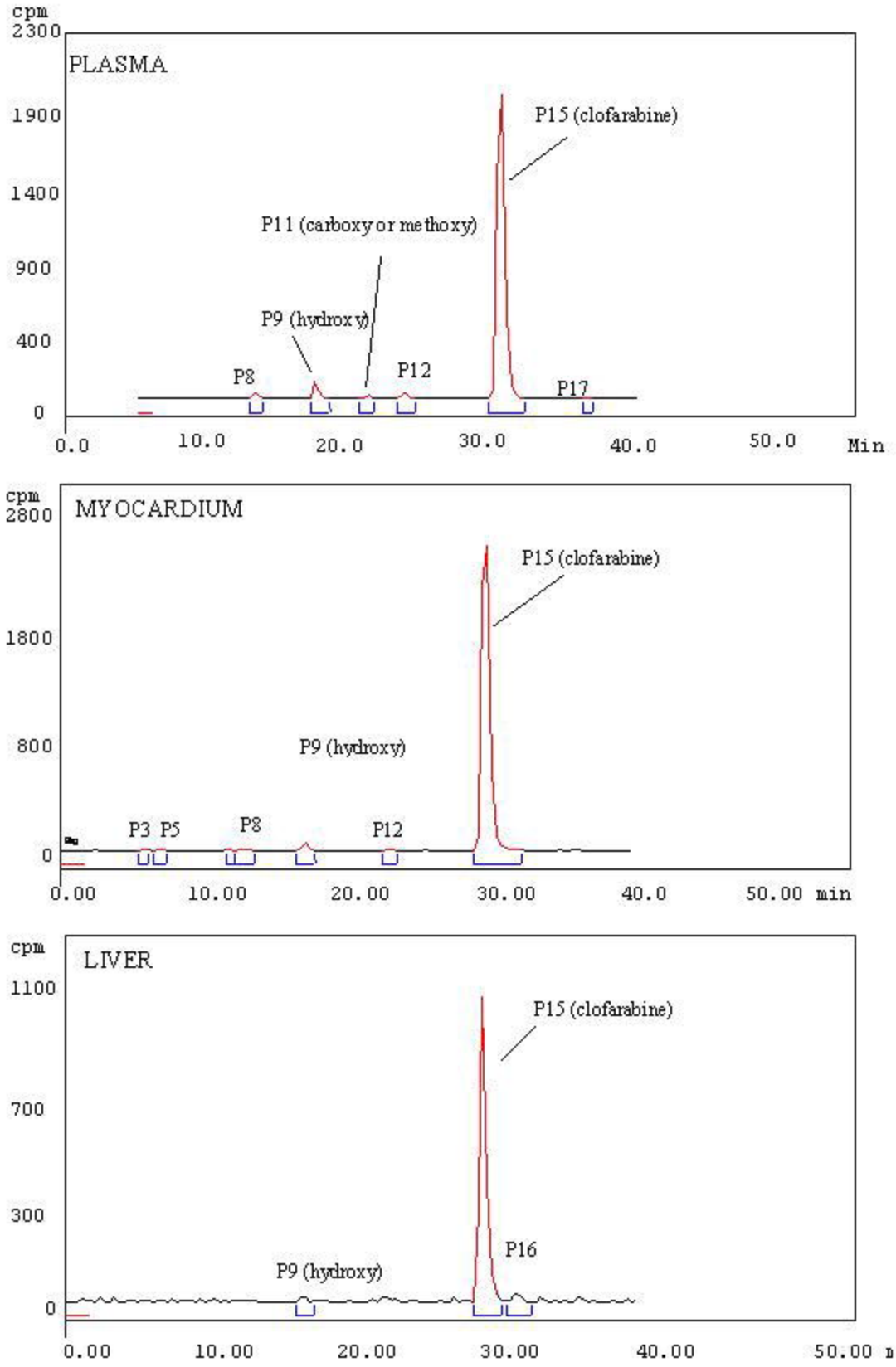

Figure 3 (2 of 2)

Figure 4

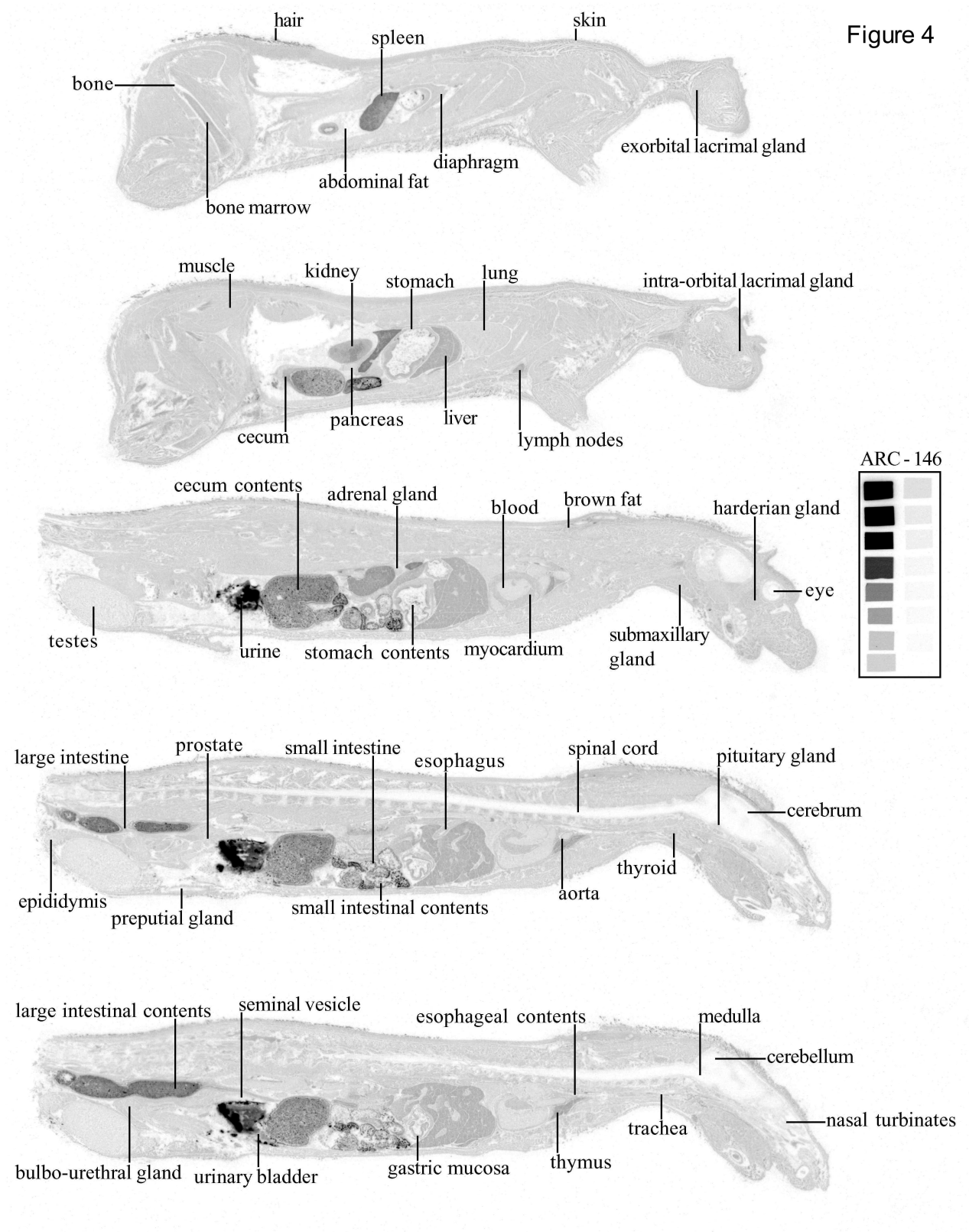
hair
spleen
skin
bone
exorbital lacrimal gland
diaphragm
abdominal fat
bone marrow
muscle
kidney
stomach
lung
intra-orbital lacrimal gland
pancreas
liver
cecum
lymph nodes
ARC - 146
cecum contents
adrenal gland
blood
brown fat
harderian gland
eye
testes
urine
stomach contents
myocardium
submaxillary gland
large intestine
prostate
small intestine
esophagus
spinal cord
pituitary gland
cerebrum
thyroid
epididymis
preputial gland
small intestinal contents
aorta
large intestinal contents
seminal vesicle
esophageal contents
medulla
cerebellum
trachea
nasal turbinates
bulbo-urethral gland
urinary bladder
gastric mucosa
thymus